Law of Mass Action, Detailed Balance, and the Modeling of Calcium Puffs

S. Rüdiger,[1] J. W. Shuai,[2,*] and I. M. Sokolov[1]

[1]*Institut für Physik, Humboldt-Universität zu Berlin, Berlin, Germany*

[2]*Department of Physics, Institute of Theoretical Physics and Astrophysics, Xiamen University, Xiamen 361005, China*

(Received 19 November 2009; published 22 July 2010)

Using deterministic-stochastic simulations we show that for intracellular calcium puffs the mixing assumption for reactants does not hold within clusters of receptor channels. Consequently, the law of mass action does not apply and useful definitions of averaged calcium concentrations in the cluster are not obvious. Effective reaction kinetics can be derived, however, by separating concentrations for self-coupling of channels and coupling to different channels, thus eliminating detailed balance in the reaction scheme. A minimal Markovian model can be inferred, describing well calcium puffs in neuronal cells and allowing insight into the functioning of calcium puffs.

DOI: 10.1103/PhysRevLett.105.048103 PACS numbers: 87.16.dj, 05.20.Dd, 05.40.−a, 87.16.dp

The assumption of well-mixedness on a given scale is crucial in many mathematical models of chemical reactions. In cellular physiology, models based on *global*, cell-averaged concentrations (reducing to systems of ordinary differential equations) reproduce, e.g., oscillations of circadian clock proteins [1]. In situations related to wave propagation in excitable media, a *local* picture is assumed leading to partial differential reaction-diffusion equations for position-dependent concentrations [2]. Both approaches rely on the mass action law. Introducing concentrations implies the existence of a domain, where molecules of all reactants are approximately homogeneously distributed. This domain must be large enough to neglect fluctuations but small compared to the length scale at which the concentrations change. Here we discuss a biochemical process on a subcellular scale, where a local concentration cannot be introduced in a useful way. Concentration gradients of one of the reactants are so steep that the assumption of mixing, here between receptor channels and their ligands, does not hold. We propose a simple representation of such reactions.

We consider localized calcium release events (puffs) associated with clusters of inositol 1,4,5-trisphosphate [IP(3)] receptor channels [3,4]. In a dual feedback loop, the channels are both stimulated and inhibited (on a slower time scale) by calcium they release from the endoplasmic reticulum (ER) [5]. The number of channels within a cluster is small and a random, stochastic opening of one of them can cause the opening of a majority of channels [6–8].

Recent high-resolution imaging [9] and computer analysis shed new light on the functionality of puffs. Reference [10] presented simulations of a cluster within realistic architecture. Because of the relatively large size of clusters [9] and rapid calcium evacuation, channels within a cluster are exposed to different calcium concentrations, thus devaluating approaches relying on mixing. We here first present a detailed computer simulation of puffs closely reproducing experimental data. The model adopts a hybrid description: While calcium concentrations are given by reaction-diffusion equations, gating transitions of channels are described within a discrete Markovian scheme. To reduce the model, we then concentrate on channels but eliminate the reaction-diffusion part by evaluating typical concentrations during release. Because of the inhomogeneous distribution of calcium, we are forced to introduce its different concentrations locally, for a direct feedback of an open channel, and at the locations of closed channels. We show that this reductional approach is capable of reproducing puffs. We further discuss that, as a consequence of imperfect mixing, the reduced model lacks detailed balance, which is a standard requirement of kinetic channel schemes. Finally, we compare characteristic properties of puff solutions to recent experiments in neuroblastoma cells.

In our simulations nine channels are placed on one surface of a cuboid [Fig. 1(a)]. Surface and cuboid represent the ER's membrane and the cytosolic space, respectively. Dynamical quantities are the concentrations of free calcium, buffers bound to calcium (dye and EGTA buffer), and the discrete states of all 36 subunits of the nine tetrameric channels. Each subunit undergoes transitions according to the standard DeYoung-Keizer (DYK) model [11]: IP(3) binding, Ca^{2+} activation binding, and Ca^{2+} inhibition binding. Transition rates between the eight subunit states were obtained by fitting experimental single channel records [12]. Details of the model and its numerical implementation can be found in the supporting material [13] and in [10,14].

Figure 1(b) shows the evolution of the number of open channels for a fixed IP(3) concentration of 0.2 μM. Channels, placed with a separation of 120 nm, open stochastically and in a cooperative manner. Accumulation of free calcium subsequently leads to inhibition of subunits and, after around 100 ms, the channels close. The duration of channel openings agrees with the duration of experimentally observed calcium puffs [9].

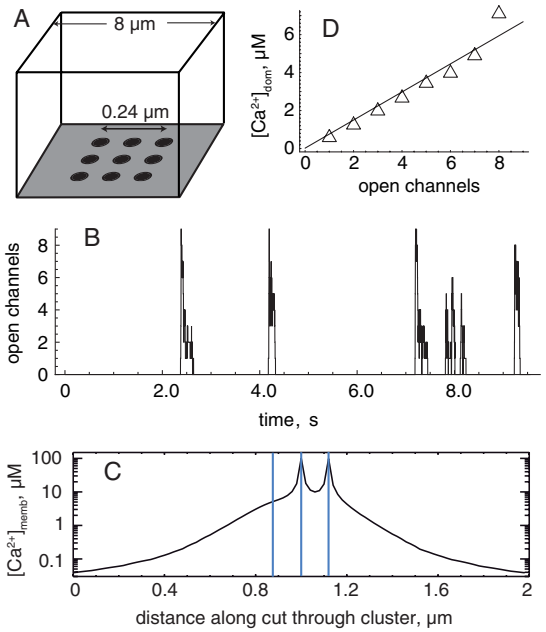

FIG. 1 (color online). Calcium release from nine channels simulated using a stochastic version of the DYK model and a deterministic reaction-diffusion scheme for Ca^{2+} and buffers. (a) The box of dimension $8 \times 8 \times 5$ μm^3 represents the cytosolic space. Channels are located in a grid on the surface (ER membrane) with calcium released into the cytosol. (b) Random puffs as cooperative openings of all or almost all channels. (c) A cut through the cluster, with vertical lines indicating the position of three channels (one is closed, two are open). (d) Calcium concentrations obtained by averaging over closed channels for a given total number of open ones.

An important open problem in the analysis of calcium signals is the determination of typical $[Ca^{2+}]$ values in the local domain of an active cluster. The magnitude of domain concentration plays a crucial role in the generation and termination of signaling events [15–18]. However, due to the properties of fluorescence imaging, the local Ca^{2+} concentrations are unclear from experimental studies, leaving the estimation of calcium levels to indirect arguments or direct numerical simulations. Recent consideration of statistical puff properties have suggested peak cluster concentrations of the order of 10 μM [18] but did not address the inhomogeneous distribution of calcium.

To determine the free calcium concentration we evaluated our direct numerical simulations and recorded $[Ca^{2+}]$ at positions of the channels. If a channel is open, large concentrations c_s of 100 μM and above are reached. However, if a channel is closed, while others are open, $[Ca^{2+}]$ assumes an intermediate value. The average of this value was defined as cluster domain concentration in [10]. Here we use a finer gradation and include the dependence of $[Ca^{2+}]$ at a closed channel on the number of open ones. If $c_i(t)$ is the Ca^{2+} concentration at the mouth of channel i at time t ($t = t_0, \ldots, t_1$) and $o_i(t)$ denotes the state of the channel (i.e., $o_i = 0$, closed; or 1, open), we define

$$c_d(n) = \sum_{i=1}^{N} \frac{1}{NT_i} \int_{t_0}^{t_1} c_i(t)[1 - o_i(t)]\delta_{nN_o(t)} dt, \qquad (1)$$

where $T_i(n) = \int_{t_0}^{t_1}[1 - o_i(t)]\delta_{nN_o(t)}dt$ is the total time when the ith channel is closed but n other channels are open, $N_o(t) = \sum_i o_i(t)$ is the number of open channels at time t, N is the total number of channels, and δ_{ij} is the Kronecker delta. The concentration $c_d(n)$ is the average concentration that a channel receives if it is closed but n other channels are open. Figure 1(d) shows that $c_d(n)$ increases linearly with n. Note that all $c_d(n)$ are considerably smaller than the concentration at the pore of an open channel (>100 μM).

Small cluster domain $[Ca^{2+}]$ results from the spatial separation of the channels and the rapid removal of calcium between the channels due to diffusion, calcium pumps, and buffer. The straight line in Fig. 1(d) represents the linear fit

$$c_d(n) = c_0 + c_1 n, \qquad (2)$$

with $c_0 = 0.02$ μM and $c_1 = 0.74$ μM. Thus, our approach leads to a large $[Ca^{2+}]$, $c_{s,0} \approx 120$ μM, for channel self-coupling and to smaller values $c = c_d(n)$ for the coupling to other channels. For calcium release from a cluster we cannot assume that reactants [IP(3)R channels and Ca^{2+}] are well mixed in the domain, since channels do not diffuse in the considered time scales [19] and the distribution of calcium ions is inhomogeneous. Therefore, the usual assumption of mass action kinetics breaks down and we are forced to consider the case of $c_s \neq c_d$ in the reaction scheme if we want to use a channel population model to discuss puff dynamics.

We further found that $[Ca^{2+}]$ values in the cluster equilibrate to c_s and c_d within milliseconds of openings or closings. We therefore consider a reduced model, in which $[Ca^{2+}]$ is given by $c_{s,0}$ and Eq. (2) but the Markovian evolution of channel states is retained. This corresponds to a coarse graining on the cluster scale and adopting different Ca^{2+} concentrations in different domains.

We first show that, due to the scale separation, the ensuing reaction scheme does not have to obey detailed balance. According to the DYK model, each channel has four subunits; each of them can bind activating and inhibiting Ca^{2+} [we ignore the IP(3) dynamics for brevity]. The state of a channel can be denoted by a four digit number, where each digit represents one of the four subunits. Each digit, in a bitwise fashion, takes on either 0 (no Ca^{2+} bound), 1 (activating Ca^{2+} bound), 2 (inhibiting Ca^{2+} bound), or 3 (both activating and inhibiting). In total there are $4^4 = 256$ states connected by transition arrows. A channel opens if at least three subunits are in state 1. Any event of binding of calcium to an open channel (e.g., the open state 0111) should be determined by the spike calcium value c_s, whereas other Ca^{2+}-binding transitions are determined by $c = c_d(n)$. Figure 2 shows a part of the transition lattice involving the open state 0111 and a

loop. Evaluating the product of rates in the clockwise and counterclockwise loop, one finds that the condition $a_5 c_d a_2 c_s b_5 b_2 = a_2 c_d a_5 c_d b_2 b_5$ necessary for detailed balance is trivially satisfied if $c_d = c_s$, but it does not hold if separation of calcium scales is assumed. We note here that the absence of detailed balance in the reduced theory is due to its coarse-grained character and represents the fact that the local equilibrium at a channel position does not correspond to a global one [20]. Invalidity of the mass action law is reflected by the two different binding rates $a_2 c_s$ and $a_2 c_d$ in Fig. 2(a), which should be contrasted with the linear rate $a_2 c$ in earlier models with detailed balance.

Figure 2(b) shows that the reduced model generates puffs of cooperated release reminiscent of the experimentally observed puffs and the puffs in our full model. What is the relevance of breaking detailed balance? To answer this question we will describe simulations with the reduced model and compare it with simulations in a related DYK model, which obeys detailed balance. Under the latter condition, we let

$$c_s(n) \equiv c_d(n) = c_0 + c_1 \frac{n}{N_{\max}}(c_{s,0} - c_0), \qquad (3)$$

which gives rest level concentration c_0 if all channels are closed, the self-coupling value $c_{s,0} = 120\ \mu M$ if all channels are open, and a linear dependence on open channel numbers. Here, we have assumed that c_1, which is a rescaled form of the parameter c_1 in Eq. (2), equals 1. In the following, however, c_1 will be a free parameter of the model.

In accordance with the estimate of cluster sizes in neuroblastoma cells in [9], we performed simulations for clusters with 5 to $N_{\max} = 10$ channels. Leaving all parameters in the determination of calcium concentrations c_d and c_s unchanged amounts to generally smaller maximal calcium concentrations for a cluster with fewer channels. For instance, a cluster of five channels where all channels are open reaches the same c_d value as a cluster of nine channels with five open channels. This treatment corresponds to keeping the cluster diameter fixed at 240 nm.

We have first calculated the distribution of peak amplitudes of puffs [Fig. 3(a)]. For these curves we have determined the maximal number of open channels during each of the events such as those in Fig. 2(b). We have first studied the case of broken detailed balance. For all channel numbers we found a strongly bimodal distribution, with many blips (single channel openings) and maximal puffs, which incorporate all of the available channels. Figure 3(b) shows a weighted average of the distributions for 5–10 channels exhibiting a peak of P_n at $n = 5$ channels. Comparison with experimental results (bars) shows good agreement in the overall distribution for puffs. However, we obtained many more blips than in the experiments (data not shown), which may be due to a higher temporal resolution, that was fixed to 1 ms in our analysis.

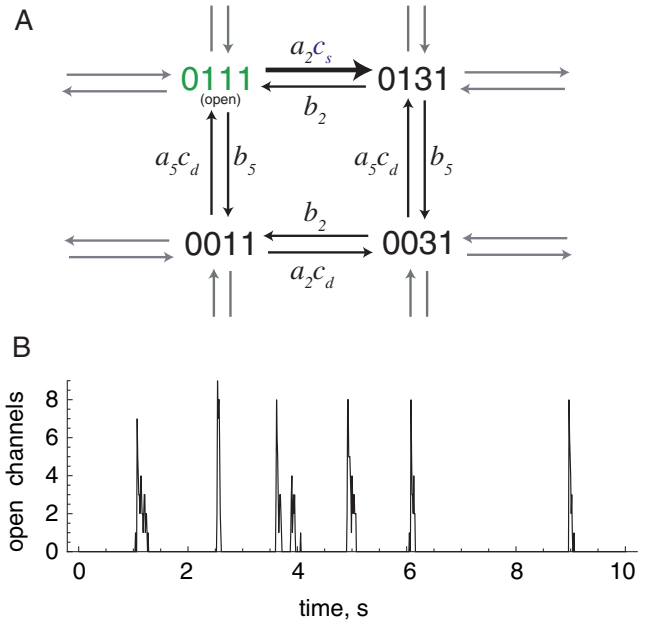

FIG. 2 (color online). (a) Exemplary loop in the transition lattice of the DYK model. Because of the separation of Ca^{2+} concentration scales, different $[Ca^{2+}]$ values appear on opposite sides of some loops involving open states. As a consequence, a net flux in the direction of the thick arrow is generated. (b) Puffs in the reduced model, where transitions are given by the DYK scheme and calcium concentrations $c_s = c_{s,0}$ and c_d given by Eq. (2).

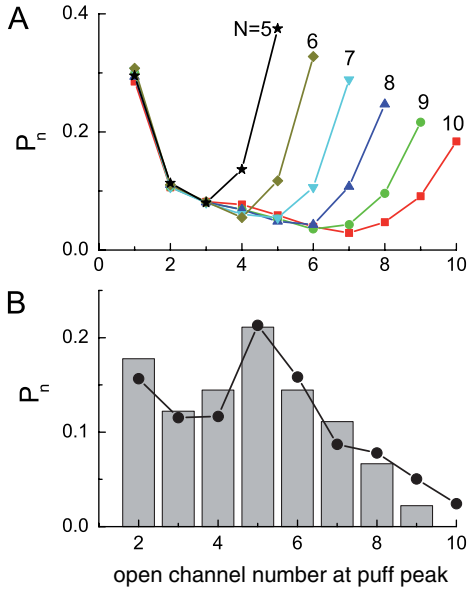

FIG. 3 (color online). (a) The distribution of puff peak amplitudes for clusters with $N = 5$–10 channels using the reduced model under conditions of broken detailed balance. Graphs in (b) are weighted averages of data as in (a). Simulations with 5–10 channels were weighted based on the experimental distribution of channels per cluster (Fig. 4C in Ref. [9]). For comparison, bars present experimental data from Fig. 4D in Ref. [9] (blips have been omitted from this analysis).

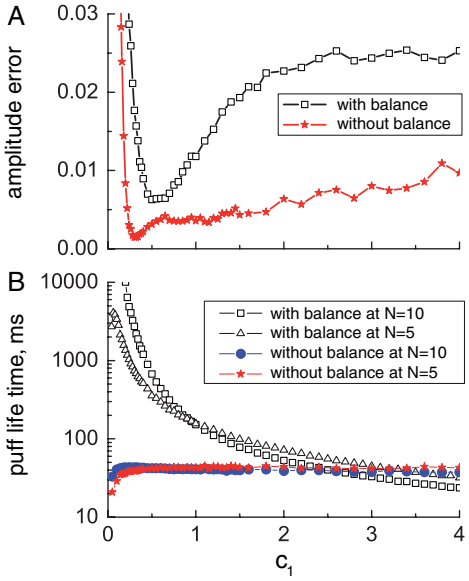

FIG. 4 (color online). (a) The deviation from the experimental puff amplitude distribution [bars in Fig. 3(b)] was calculated for models with and without detailed balance using the error sum $\sum_{i=2}^{10}(P_n - P_{n,\mathrm{exp}})^2$. (b) The puff lifetime (average for events with more than one channel opening) is constant over a large range of parameter c_1 for the broken detailed balance model (circles and stars). For models with Eq. (3) realistic lifetimes can be achieved for c_1 larger than 1 only (see open boxes and triangles), which implies increased binding site concentrations c_s larger than 120 μM.

We next compared our model with models obeying detailed balance by fitting them to experimental data of two of the best studied puff properties. Our goal was an optimum for varying the parameter c_1 in Eqs. (2) (broken balance) and (3) (balance). The parameter c_1 represents the effective separation of channels and depends, for instance, on the concentration of mobile buffer [10]. Figure 4 shows the models' errors in peak distributions [difference between bars and dots in Fig. 3(b)] and puff lifetime. Puff lifetime has been obtained as full duration at half maximum and should be compared to experimental values of around 50 ms [9]. The best agreement can be found for the case of broken detailed balance for c_1 around 0.3. However, for the model (3) it is impossible to obtain both short puffs and a realistic amplitude distribution for the same parameter value c_1.

In summary, we have described how the standard coarse-graining approach fails for strongly localized biochemical processes. An assumption of well-mixedness does not hold since concentration gradients of reactants are very steep. For a correction, we suggest to separate concentration scales into large open channel values and smaller concentrations at closed channels. We obtain a reduced Markovian model, which replicates temporal spikes in the reaction very well. Importantly, the scale separation leads to a breakdown of detailed balance on the coarse-grained level of channel gating models. By comparison of our results with experimental data we identified the relevance of breaking the detailed balance. First, in order to fit the patch clamp data for isolated channels [12], inhibition occurs at large Ca^{2+} concentrations (dissociation constant $d_2 = 50\ \mu M$, see supporting material [13]). For a model with detailed balance, however, cluster domain concentrations are too small for inhibition if c_1 is small, resulting in too long puffs. On the other hand, if c_1 is large ($c_1 > 2$), one can find short puffs, but now c_s is large already for small numbers of open channels, effectively suppressing large amplitude puffs. This problem does not occur in models with broken detailed balance, which provide two different Ca^{2+} scales for puff activation and termination. Therefore, our approach facilitates the robust generation of short puffs with large peak amplitudes. These results are crucial in understanding localized calcium signals, which are a basic part of many cellular signaling processes, for instance, in neurons or muscle cells.

S. R. and I. S. acknowledge support from the DFG within program SFB 555. J. S. has been supported by the NSF China under Grant No. 10775114 and the NIH U.S. under Grant No. 2RO1GM065830-06A1.

*jianweishuai@xmu.edu.cn

[1] J. Keener and J. Sneyd, *Mathematical Physiology: Cellular Physiology* (Springer, New York, 2008).
[2] B. Pando, J. E. Pearson, and S. P. Dawson, Phys. Rev. Lett. **91**, 258101 (2003).
[3] I. Parker, J. Choi, and Y. Yao, Cell Calcium **20**, 105 (1996).
[4] R. Thul and M. Falcke, Phys. Rev. Lett. **93**, 188103 (2004).
[5] M. Bär *et al.*, Phys. Rev. Lett. **84**, 5664 (2000).
[6] S. Swillens *et al.*, Proc. Natl. Acad. Sci. U.S.A. **96**, 13 750 (1999).
[7] J. W. Shuai and P. Jung, Phys. Rev. Lett. **88**, 068102 (2002).
[8] M. Falcke, Adv. Phys. **53**, 255 (2004).
[9] I. F. Smith and I. Parker, Proc. Natl. Acad. Sci. U.S.A. **106**, 6404 (2009).
[10] S. Rüdiger *et al.*, Biophys. J. 99, 3 (2010).
[11] D. W. DeYoung and J. Keizer, Proc. Natl. Acad. Sci. U.S.A. **89**, 9895 (1992).
[12] J. W. Shuai *et al.*, Chaos **19**, 037105 (2009).
[13] See supplementary material at http://link.aps.org/supplemental/10.1103/PhysRevLett.105.048103 for a description of model and numerical methods.
[14] S. Rüdiger *et al.*, Biophys. J. **93**, 1847 (2007).
[15] G. Ullah and P. Jung, Biophys. J. **90**, 3485 (2006).
[16] G. Ullah, P. Jung, and K. Machaca, Cell Calcium **42**, 556 (2007).
[17] H. DeRemigio, J. R. Groff, and G. D. Smith, Math. Med. Biol. **25**, 65 (2008).
[18] D. Swaminathan, G. Ullah, and P. Jung, Chaos **19**, 037109 (2009).
[19] I. F. Smith *et al.*, Sci. Signal. **2**, ra77 (2009).
[20] V. Nguyen, R. Mathias, and G. D. Smith, Bull. Math. Biol. **67**, 393 (2005).

Supporting Material
Law of mass action, detailed balance, and the modeling of calcium puffs

S. Rüdiger
Institute of Physics,
Humboldt-Universität zu Berlin, Germany,
J.W. Shuai
Department of Physics,
and Institute of Theoretical Physics and Astrophysics
Xiamen University, China
I.M. Sokolov
Institute of Physics,
Humboldt-Universität zu Berlin, Germany,

In this supporting material we provide a detailed description of our hybrid stochastic/deterministic model as well as a sketch of the numerical methods we used.

S1. Model equations

Partial differential equations for the concentration fields (multi-channel simulations)

The calcium concentration in the cytosol is determined by diffusion, transport of calcium through the ER membrane, and binding and unbinding of calcium to buffer molecules. In the cytosol we consider the following types of buffers: exogenous mobile buffer with fast or slow reaction kinetics and a stationary buffer with fast kinetics.

Buffers are assumed to be distributed homogeneously at initial time. Total concentrations of mobile and dye buffers are denoted by B_m and B_d, while the concentrations of corresponding buffer bound to calcium are denoted by b_m and b_d, respectively, which are determined by mass-action dynamics:

$$\frac{\partial c}{\partial t} = D\nabla^2 c - k_m^+(B_m - b_m)c + k_m^- b_m - k_d^+(B_d - b_d)c + k_d^- b_d, \quad (1)$$

$$\frac{\partial b_m}{\partial t} = D_m\nabla^2 b_m + k_m^+(B_m - b_m)c - k_m^- b_m, \quad (2)$$

$$\frac{\partial b_d}{\partial t} = D_d\nabla^2 b_d + k_d^+(B_d - b_d)c - k_d^- b_d. \quad (3)$$

Here, the $k^\pm$ denote the on and off rates of calcium reacting with the corresponding buffer proteins. Parameters for the mobile and dye type of buffers used for this work are listed in Tab. S1. The equations are solved in a rectangular box domain bounded on one side by an idealized quadratic membrane patch of $(8+3\times d)$ μm side length, where d is the distance between the channels. In the z-direction, perpendicular to the membrane, we consider a spatial extent of $5\,\mu$m. All boundary conditions except for c at the ER membrane are no-flux conditions. The boundary condition for c at the membrane models the transport through the membrane,

$$D\partial_z c = -J, \text{ at } z = 0 \quad (4)$$

and comprises three contributions:

$$J = P_c S(\vec{r}, t)(E - c) - P_p \frac{c^2}{K_d^2 + c^2} + P_l(E - c), \quad (5)$$

where $\vec{r} = (x, y, 0)$ denotes the position on the membrane. Calcium moves from the ER to the cytosol through IP_3 receptors and by a small leak contribution, which are modeled by terms with coefficients P_c and P_l, respectively. In the other direction calcium is resequestered into the ER by pumps (P_p). The action of pumps is assumed to be cooperative in calcium and modeled with a quadratic c dependence. K_d is the dissociation constant of the pumps. The first term in Eq. 5 represents the current through the channel, where P_c is adjusted such as to represent a total current of 0.1 pA if the channel is open. We model the source area of a channel by a circle of radius $R_s = 6$ nm (1). The positions of channels in the rectangular box are given by $\vec{X}_{kl} = ((4 + (k + 1/2)d)\,\mu\text{m},\ (4 + (l + 1/2)d)\,\mu\text{m},\ 0)$, where k and l run from 0 to 2. The channel flux term in Eq. 5 is controlled by the channel state through the factor $S(\vec{r}, t)$,

which is defined by:

$$S(\vec{r},t) = \begin{cases} 1, & \text{if there is an open channel } (k,l) \text{ and } \left\|\vec{r} - \vec{X}_{kl}\right\| < R_s, \\ 0, & \text{otherwise.} \end{cases}$$

For a more detailed description of the membrane current modeling we refer to (2). The parameters that we use in the current work are shown in Tables S1 and S2.

S2. Numerical methods

S2.1 Multi-channel setup

Our numerical method consists of coupled solvers for the deterministic set of PDEs and the stochastic equations. In view of the multiple scales in length and time we employ a conforming finite element method for the spatial discretization and an adaptive linear implicit time-stepping for the deterministic part. The stochastic solver is based on the Gillespie method (3), which is adaptive in the sense that its time step follows the evolution of transition probabilities. A complication arises since the usual Gillespie method solves stochastic processes where the transition rates are constant during subsequent transitions. However, for channels with Ca^{2+} as carrier the rates may change rapidly due to channel openings and closings. This problem was solved by devising the hybrid method described in (2), where we introduced and tested the hybrid method for a single channel system—here the obvious generalization to multi-channel systems will be used.

We discretized the spatial domain by linear finite elements (4). The attractive feature of the method is its ability to effectively handle complex geometries. For our simulations of release from clustered channels we employ a grid with a very fine resolution in the channel area. There the grid length is around 0.3 nm. With increasing distance from the channel the grid is coarsened up to 1600 nm.

S2.2 Stochastic model of channel gating

To incorporate the open/close dynamics of a single or multiple IP_3Rs we adopt the DeYoung-Keizer model (6, 7). According to the DeYoung-Keizer model, an IP_3R consists of four identical subunits. There are three binding sites on each subunit: An activating site for Ca^{2+}, an inhibiting Ca^{2+} site, and an IP_3 binding site. The three binding sites allow for 8 different states X_{ijk} of each subunit. The index i indicates the state of the IP_3 site, j the one of the activating Ca^{2+} site and k the state of the inhibiting Ca^{2+} site. An index is 1 if a Ca^{2+} ion or IP_3 is bound and 0 if not. Rates of transitions involving binding of a molecule are proportional to the concentration of the respective molecule.

We associate nine stochastic variables $X_{000}(i)$, $X_{001}(i)$, ..., to each channel i. These variables count the numbers of subunits of channel i that are in the respective state. That is, each variable can take on values from 0 to 4, while the sum of all nine variables for each channel must equal 4. The Ca^{2+} concentration for the activation and inhibition processes are evaluated at the channel center position. In the multi-channel simulations this value for an open channel reaches 110 μM.

References

1. Thul, R., and M. Falcke, 2004. Release currents of IP_3 receptor channel clusters and concentration profiles. *Biophys.J.* 86:2660–2673.

2. Rüdiger, S., J. Shuai, W. Huisinga, C. Nagaiah, G. Warnecke, I. Parker, and M. Falcke, 2007. Hybrid Stochastic and Deterministic Simulations of Calcium Blips. *Biophys. J.* 93:1847–1857.

3. Gillespie, D. T., 1977. Exact Stochastic Simulation of Coupled Chemical Reactions. *J. Phys. Chem.* 8:2340.

4. Nagaiah, C., S. Rüdiger, G. Warnecke, and M. Falcke, 2008. Adaptive numerical simulation of intracellular calcium dynamics using domain decomposition methods. *Applied Numerical Mathematics* 58:1658.

5. Shuai, J., J. E. Pearson, J. K. Foskett, D. D. Mak, and I. Parker, 2007. A Kinetic Model of Single and Clustered IP_3 receptors in the Absence of Ca2+ Feedback. *Biophys. J.* 93:1151–1162.

6. DeYoung, G., and J. Keizer, 1992. A single-pool inositol 1,4,5-trisphosphate-receptor-based model for agonist-stimulated oscillations in Ca^{2+} concentration. *Proc.Natl.Acad.Sci USA* 89:9895–9899.

7. Keizer, J., and G. DeYoung, 1994. Simplification of a realistic model of IP_3-induced Ca^{2+} oscillations. *J.theor.Biol.* 166:431–442.

8. Dargan, S., and I. Parker, 2003. Buffer kinetics shape the spatiotemporal patterns of IP_3-evoked Ca^{2+} signals. *J.Physiol.* 553:775–788.

9. Smith, I., and I. Parker, 2009. Imaging the quantal substructure of single IP3R channel activity during Ca2+ puffs in intact mammalian cells. *Proceedings of the National Academy of Sciences* 106:6404.

10. Allbritton, N., T. Meyer, and L. Sryer, 1992. Range of messenger action of Calcium ion and inositol 1,4,5 trisphosphate. *Science* 258:1812–1815.

Buffer	**parameter**	**value**	**unit**
slow buffer (EGTA)			
	k_m^+	6 (8)	$(\mu\text{M s})^{-1}$
	k_m^-	1 (8)	s^{-1}
	D_m	95	$\mu\text{m}^2\text{s}^{-1}$
	B_m	800	μM
dye buffer			
	k_d^+	150	$(\mu\text{M s})^{-1}$
	k_d^-	300	s^{-1}
	D_d	20	$\mu\text{m}^2\text{s}^{-1}$
	B_d	25	μM

Table S1. List of buffer kinetic parameters. Numbers in brackets denote references where specific values have been taken from.

Parameter	**symbol**	**value**	**unit**
diffusion coefficient			
free Ca^{2+}	D_c	223 (10)	$\mu m^2 s^{-1}$
membrane transport parameters			
channel flux coefficient	P_c	6.32×10^6	nm s^{-1}
pump flux coefficient	P_p	400000	nm μM s^{-1}
leak coefficient	P_l	5.658	nm s^{-1}
8-state model			
IP_3-binding			
	a_1	1000	$(\mu M\ s)^{-1}$
	a_3	500	$(\mu M\ s)^{-1}$
	d_1	0.005	μM
	d_3	0.2	μM
activating Ca^{2+}			
	a_5	100	$(\mu M\ s)^{-1}$
	d_5	0.2	μM
inhibiting Ca^{2+}			
	a_2	0.1	$(\mu M\ s)^{-1}$
	a_4	0.1	$(\mu M\ s)^{-1}$
	d_2	50	μM
	d_4	1.25	μM
pump-dissociation coefficient	K_d	0.2 (1)	μM
Ca^{2+} concentration in ER	ER_{const}	700 (1)	μM
IP_3 concentration		0.2	μM

Table S2. List of parameters used for our model. The on-rates a_i, off-rates b_i and the dissociation constants d_i are related by $d_i = b_i/a_i$. In the third column, numbers in brackets denote the reference paper.